# AguaClara SRSF-Bench Scale

Danhong Luo, Weiling Xu, Huifei Wu, Main Editor: Michael Adelman

May 17, 2012

**Abstract**

Stacked rapid sand filtration (SRSF) is a novel technology for AguaClara water treatment plants. Our team goal is to improve the performance of the SRSF by studying fundamental questions such as the self-healing nature of flow distribution among layers and the effect of upstream energy dissipation rate on performance. In the self-healing test, we found that it is hard to let the sand bed itself control what the flow distribution will be, and that surface removal dominated in the filtration process. The depth filter test reveals that surface removal dominated in the self-healing test, and flow distribution improved when surface removal effects were eliminated. For the energy dissipation rate test, we assume the filter performance would be improved with the increasing energy dissipation rate, while current experiments have not show the result. Therefore, further testing should be addressed in the energy dissipation rate study.

## Background

Stacked rapid sand filtration is a novel technology for AguaClara water treatment plants, which compared to conventional filters requires less water to backwash, as well as a smaller footprint to achieve the same level of filtration. In order to improve the performance of stacked rapid sand filtration, and the possibility to scale it according to the needs in the field, having a clearer understanding behind the filtration process, especially what are the hydraulics characteristics if different sand grains are implemented, is an important step.

For conventional filters, granular materials including sand, anthracite coal, magnetite, and garnet sand are usually used. The surface small sand often serves as a "surface filter," which could remove the particles that are larger than the pore size; and the larger sand worked as a "depth filter," where particulates were captured within a porous body of material. The filtration approach velocity is approximately 0.7 mm/s to 2.8 mm/s, and the backwash approach velocity is around 10 mm/s to 13 mm/s, which is similar in size to AguaClara sedimentation tank[1].

Uneven flow among layers of the stacked filter would be a significant operational problem. The hydraulic design and sand media selection for a stacked filter must account for proper distribution of flow in the filter but there is little

data to support design guidelines for either of these. We initially hypothesized that uneven sand gradation would lead to coarser and finer layers of the filter, and we would like to know how much of a problem this would be and how quickly it may correct itself.

In addition, according a study about designing granular filters, there should be linear increasing relationship between head loss and volume of filtrate when filters are operating at a constant rate. When the curve of head loss versus volume is convex, it reveals that surface rather than depth removal of solids is taking place and higher filter rates may be needed. On the other side, if the curve is concave, it shows weak removal of solids and potential passage of turbidity during constant rate filtration. [2]

For the relationship between energy dissipation rate $\varepsilon$ and floc size which has been widely studied, the past works show that the energy dissipation rate would influence the floc aggregation as well as the breakup process. In the study by Tse et al. (2011), it shows that the high energy dissipation rate will increase the collision frequency and hence create large floc aggregates quickly; but on the other hand, a higher $\varepsilon$ will break up large flocs. The best results in terms of turbidity removal require a combination of low energy dissipation rate and long residence time. The more efficient removal of colloids at low $\varepsilon$ could be due to the creation of large flocs that have a higher sedimentation velocity, which could increase their ability to collide with other colloids.[3] Parker et al. (1972) found that the maximal floc diameter is related to the dissipation rate of the kinetic energy according to $d \propto \varepsilon^{1/4}$, whatever the floc size in relation to the Kolmogorov microscale. Kobayashi et al. (1999) modeled the floc as a heterogeneous medium, composed of a finite number of primary particles. They found the same result as did Parker et al. (1972). The expressions of Tambo and Ozumi (1978) are slightly different because they considered the floc fractal dimension. In the viscous sub range, they related the maximal floc diameter to the dissipation rate of the kinetic energy according to$d \propto \varepsilon^{a}$, where $0.33 \leq a \leq 0.38$. In the inertial sub range, the relation is given by $d \propto \varepsilon^{b}$, where $0.4 \leq b \leq 0.5$.[4]

# Experimental Design

## Flow Distribution Tests

The experiments was conducted with two 2.5 cm diameter columns with full process control for chemical feeds, backwash, and turbidity measurements. The experimental setup followed the steps below:

1. Set up two clear PVC pipe columns with proper adapters and screens.
2. Connected plumbing and solenoid valves as shown in the process flow diagram below.
3. Installed and calibrated flow sensors to log the flow rate in each filter during the course of this test.

4. Set up Process Controller to log the experimental data .

5. Tested the hydraulics of the system by filling the two columns with identical filter sand and verifying that the flow is evenly distributed.

6. Sieved sand in the soils lab and added a coarse fraction and fine fraction to the two columns

The general experiment apparatus is shown in Figure 1. Depending on the goal of what we are looking for, we have performed two tests, equal sand test and unequal sand test. For the equal sand test, our goal was to validate the other elements of the plumbing, as well as study the influence of hydraulic disturbances. Therefore, we filled both columns with 250 g of typical rapid sand filtration sand ($d_{eff} = 0.5mm$ and $C_U = 1.4$). For the unequal sand test, our goal was to study the influence of hydraulic conductivity. Therefore, we filled both columns with equal height of sand, and the masses for Column 1 and Column 2 are 160 g and 158 g respectively.

The experiment runs with a few hours of clean flow to steady state before adding clay and alum to the system.

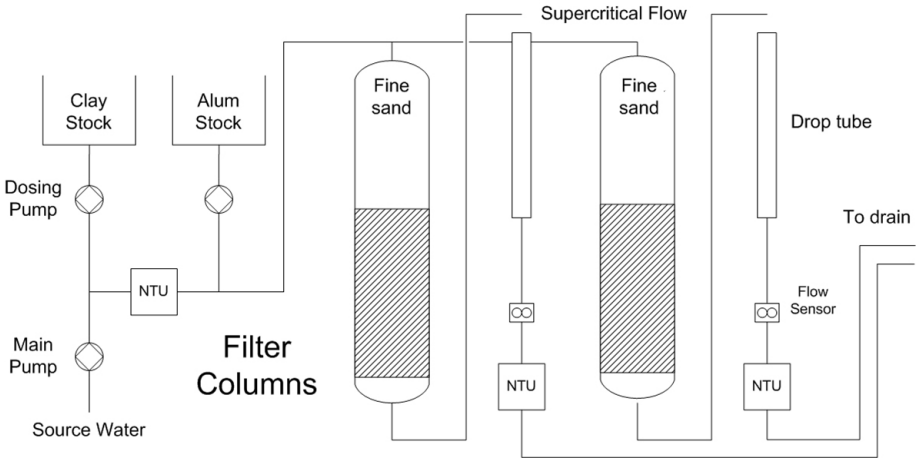


Figure 1: Flow distribution test setup

## Depth Filtration Test

The flow distribution test #5 result gave parabolic-shaped time versus head loss curves (Figure 16), which indicated that the surface removal dominated the filter process. In order to study the effect of depth filtration, we modified the general experiment apparatus by insert the incoming pipe into the sand layer, to eliminate the effect of surface removal (Figure 2).

The apparatus runs in the same setup as the flow distribution test.

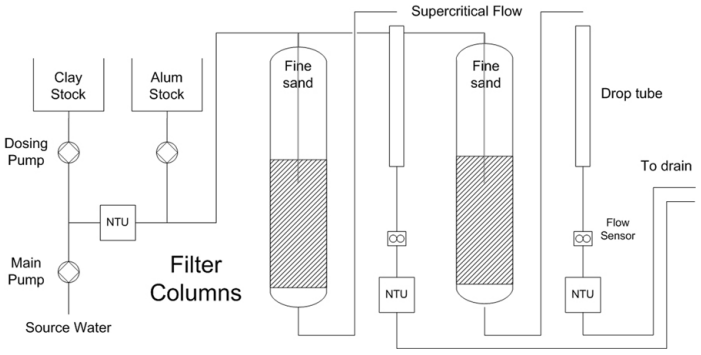


Figure 2: Depth filtration test setup

## Energy Dissipation Rate Study

Recent field study found that the SRSF in Tamara performs very well. Comparing the Tamara plant to the stacked filters tested in the laboratory, we hypothesize it is the flocculator upstream of the filter at the Tamara plant that contributes to the better filter effect of Tamara compared to data from the lab. Filtration theory predicts that if incoming particles are even slightly larger than the typical primary particle size of suspended clay (1 $\mu m$), the performance of the filter will improve significantly. In order to verify this assumption, we ran the energy dissipation rate study.

Based on the previous apparatus, we added a tube flocculator at the beginning of the system, and using a needle valve to change the energy dissipation rate to control the floc size. In order to form relatively big floc before the needle valve, we increased the stock alum concentration to $XX^{\mathrm{mg}/\mathrm{L}}$. To eliminate the surface removal effect and simplify the setup, up flow filter mode was used in this test (Figure 3).

The theoretical energy dissipation rate could be calculated through equation (1):

$$\varepsilon_{Max} \cong \frac{\Pi_{Jet} \cdot V_{Jet}}{D_{Jet}} \tag{1}$$

where, $D_{Jet}$ could be solved for from the column head loss as an effective orifice diameter, $V_{Jet}$ could be estimated from the needle valve head loss, and $\Pi_{Jet}$ is the jet coefficient, which is about 0.62.

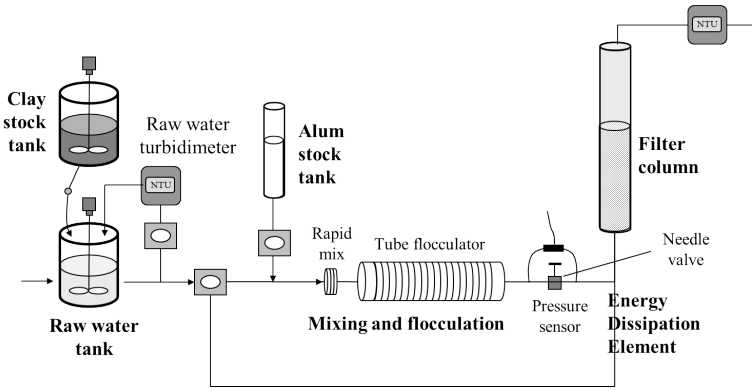


Figure 3: Energy dissipation study setup

### Sand Preparation

The sands used in the experiment are typical rapid filtration sands. We passed the typical rapid filtration sand through a #30 soil sieve, putting the coarse fraction in one column and the fine fraction in the other column.

## Results and Discussion

### Flow Sensor Calibration

From Michael Adelman's previous study, we got the flow sensor calibration to convert the flow sensor reading ($cm$) into the actual flow rate ($^{\text{mL}}/_{\text{min}}$) (Figure 4).

Sensor 1

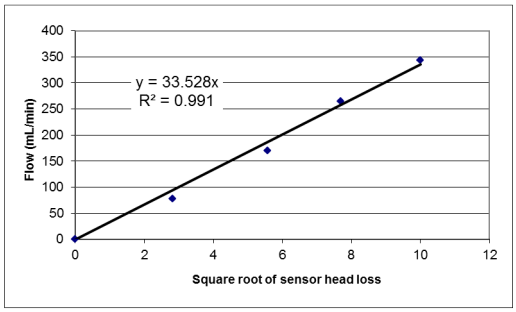


Sensor 2

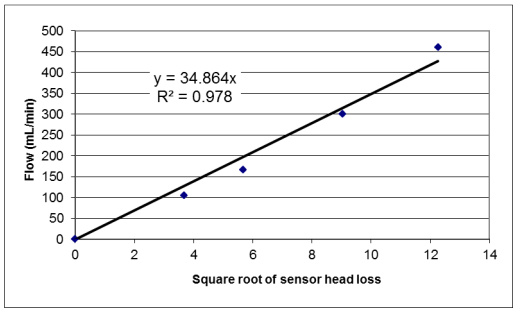


Figure 4: Flow sensor calibration

## Equal Sand Tests

### Result 1

These batches of experiments ran for 5 hours with clean incoming water and 20 hours with 20 NTU raw water and alum. Since both of them ran under the same conditions, we discuss the results together.

Shown in Figure 5, at the first trial, Column 1 became over-loaded after 20 hours test, while Column 2's effluent turbidity was still under-loaded. But at the second trial, both columns generate a low effluent turbidity after 20 hours.

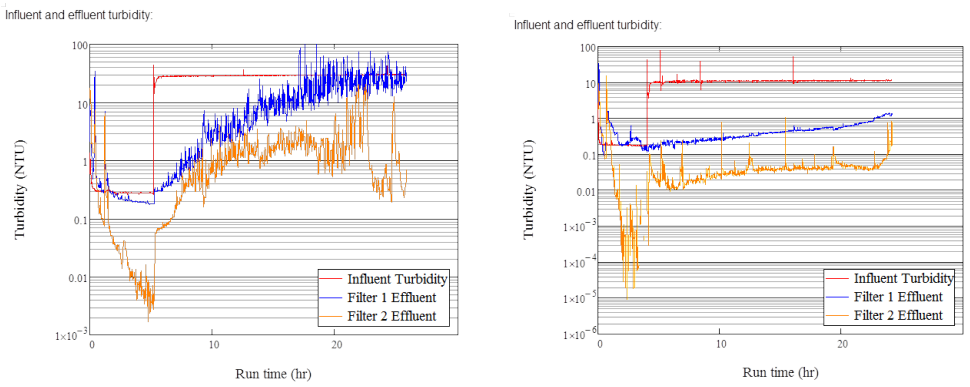


ID Tag 2 ID Tag 3

Figure 5: Turbidity of both columns of Result 1 for Equal Sand test

Shown in Figure 6, there was an obvious uneven distribution of the flow rate in Column 1 and Column 2, which is different from what we expected. This perhaps was caused by the different water yields in the two columns. The sum of both flow rates stays constant, which is consistent with the steady total incoming flow rate.

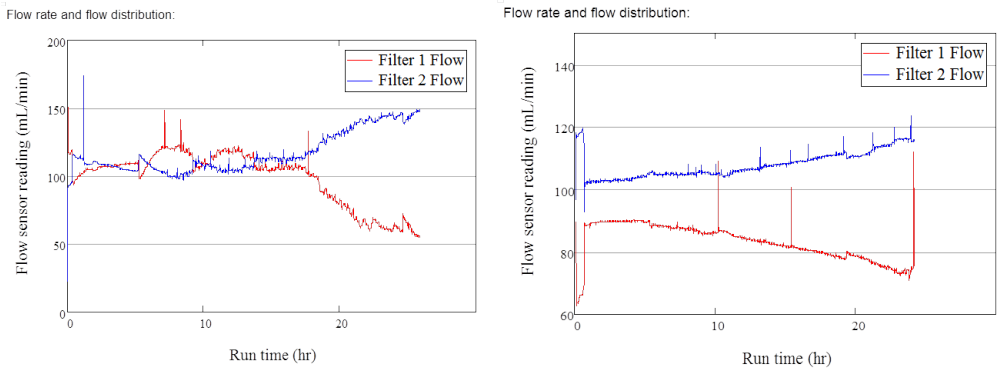


ID Tag 2 ID Tag 3

Figure 6: Flow rate of both columns of Result 1 for Equal Sand test

The head losses of both columns (Figure 7) had the same trend as run time went by. Especially for the first trial, at the run time at near 20 hour, there was a sudden decrease in both two columns. We suppose that there might be a sudden shock at that time, correspondingly, the head loss in two columns dropped at that time. There was also a tendency to converge as filtration process continues.

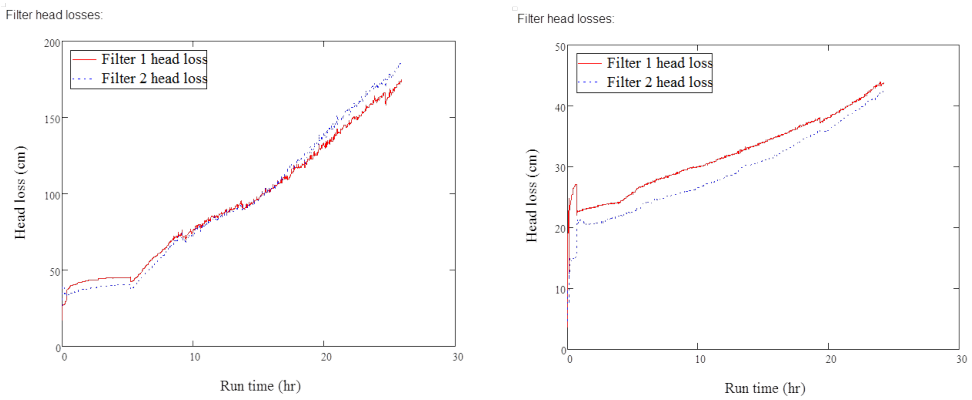


Figure 7: Head loss of both columns of Result 1 for Equal Sand Test

**Result 2 (Perturbation Test)**

This experiment ran 1 hour with clean incoming water for the perturbation test, and ran another 18 hours with 5 g/L clay stock added to produce 20 NTU influent, and 1.5 mg/L alum added as a coagulant.

Figure 8 and Figure 9 show the flow distribution and the head loss in two columns for the perturbation test. According to the experiment records and Figure 8, when Column 1 was hit, the flow rate in Column 1 displayed a sudden increase and then decreased to the normal level, and the head loss experienced a corresponding decrease and increase. As we supposed before, the flow rate in Column 2 acted in response to the perturbation in Column 1, which dropped rapidly and increased back to the normal level. The same phenomenon occurred if we hit Column 2.

It should be noted that, after hitting a particular column, the flow rate in that column increased. This maybe the sand became compressed after being perturbed. In order to make the following experiment ran under the same condition, we hit the two columns in pairs.

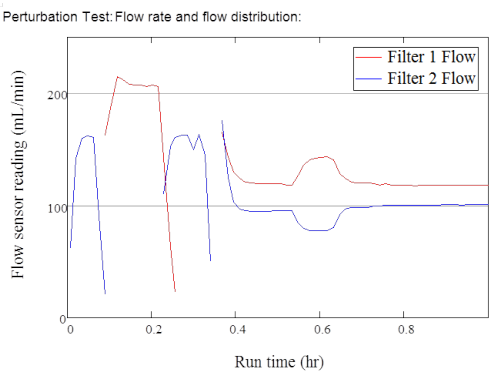


Figure 8: Flow rate of both columns of Result 3 for Equal Sand Perturbation test

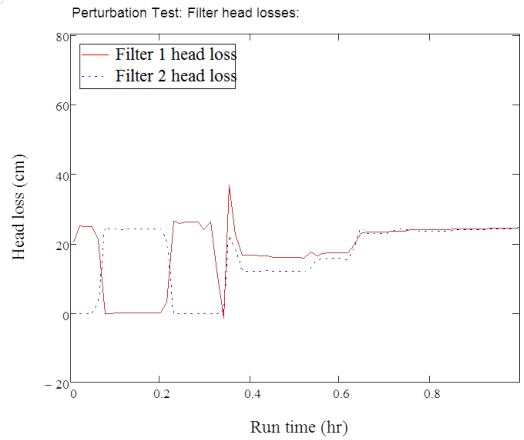


Figure 9: Head loss of both columns of Result 3 for Equal Sand Perturbation test

Figure 10, 11 and 12 shows the result for an 18 hour test with 20 NTU influent as described previously. According to Figure 9, the effluent turbidity in Column 1 got close to the influent turbidity after 10 hours, from which we could infer that Column 1 became over-loaded after running for 10 hours' test. However, the effluent turbidity in Column 2 decreased gradually during the experiment, which showed that Column 2 still worked well after 19 hours. This situation might be explained by the different flow rate distribution in two columns. From Figure 11, we could see that the flow rate in Column 1 increased with the run time, but in Column 2, it decreased with the run time. It might be the high flow rate introduced more clay to the column, that caused the earlier overloading in Column 1 than Column 2.

The head losses in two columns (Figure 12) were very close with as run time went by. After 10 hours' running, the head loss in Column 2 was a little higher than Column 1, but both of them showed a clear and similar trend.

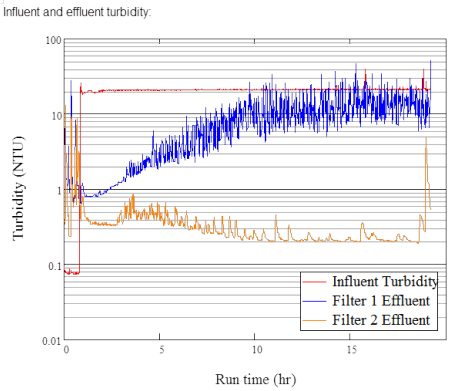


Figure 10: Turbidity of both columns of Result 2 for Equal Sand test

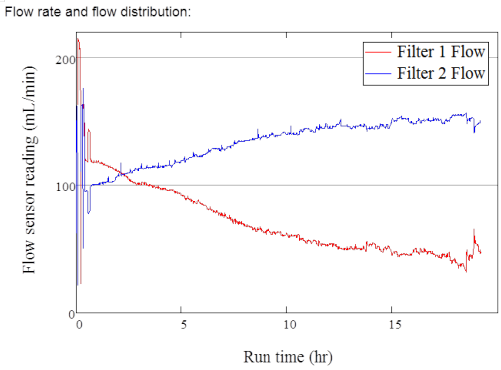


Figure 11: Flow rate of both columns of Result 2 for Equal Sand test

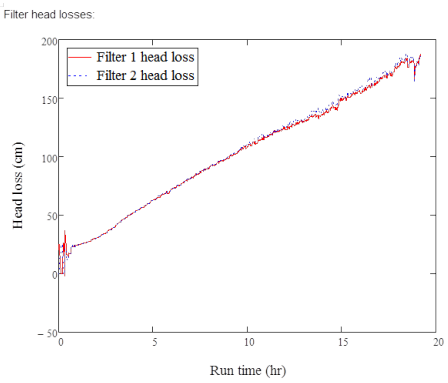


Figure 12: Head loss of both columns of Result 2 for Equal Sand test

**Result 3**

These batches of tests ran with 20 NTU raw water for 44 hours and 14 hours respectively. Since both of them ran under the same conditions, we discuss the results together.

According to Figure 13, the influent turbidity kept relatively constant at 20 NTU in two cases, and the effluent turbidity in two columns displayed the same increasing trend in two tests. Both tests showed that the average effluent turbidity in Column 1 approached the influent turbidity at about 20 hours, which allows us to infer that Column 1 was overloaded after 20 hours' running.

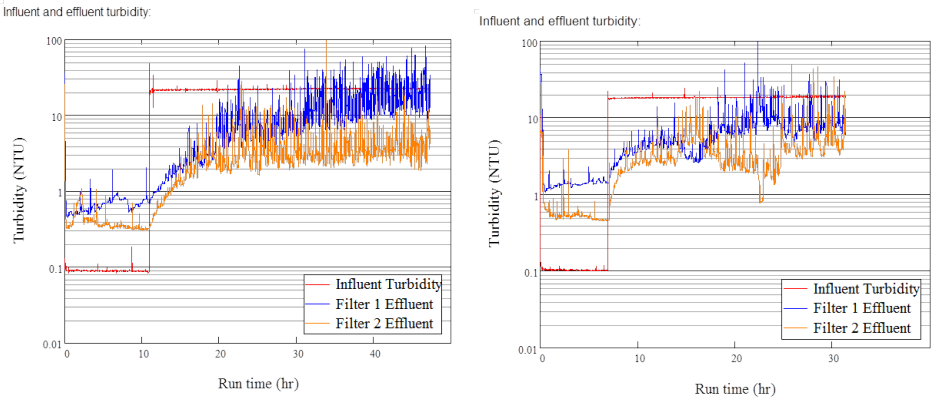


Figure 13: Turbidity for three tests of Result 3

Figure 14 showed the flow rate with the run time. In test 8 (ID Tag 8), the flow rate in two columns displayed an "X" shape, which means they converged at first, and diverged after a certain time. While in test 9 (ID Tag 9), the flow

rate kept constant all the time. This result is interesting, because two tests ran under the same condition, but the flow rate distribution had a totally different trend.

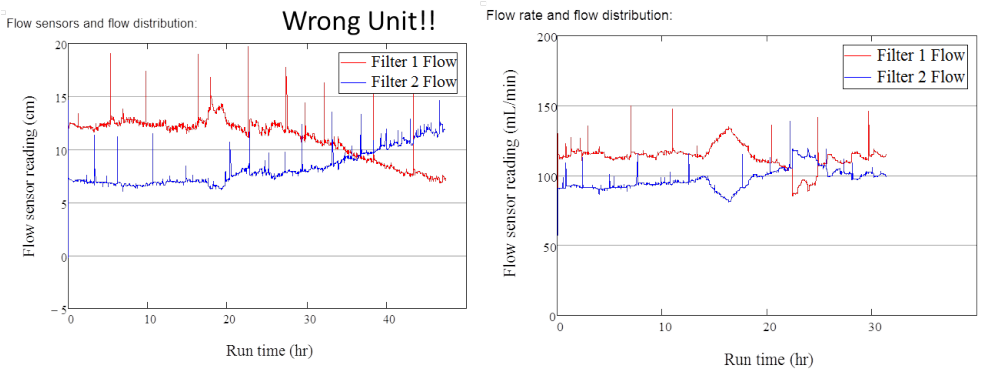


ID Tag 8 ID Tag 9

Figure 14: Flow rate distribution for three tests of Result 3

Figure 15 showed the head losses in two tests. Both of them had the same trend.

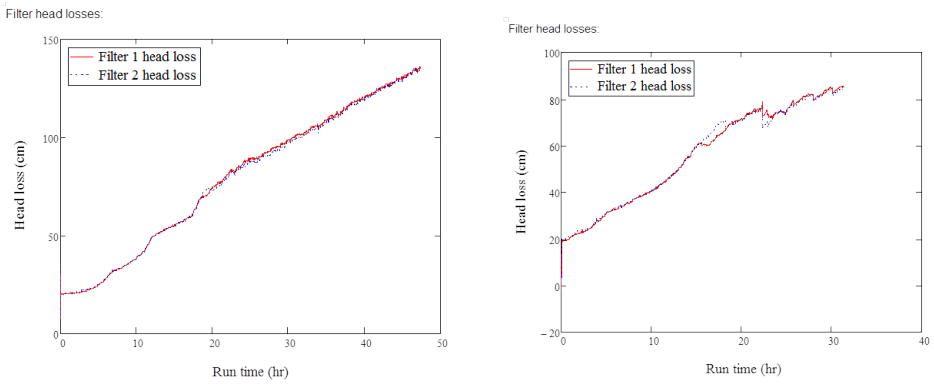


ID Tag 8 ID Tag 9

Figure 15: Head loss for three tests of Result 3

**Result 4**

This experiment ran with 20 NTU raw water and 1.5 mg/L alum as coagulant for 45 hours.

Shown in Figure 16, the effluent turbidity got close and exceeded to the

influence turbidity after 40 hours' running. Compared with Result 4, it indicates the coagulant improved the filter capacity.

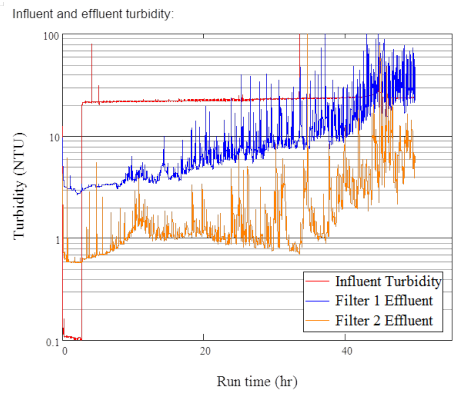


Figure 16: Head loss of both columns of Result 4 for Equal Sand test

Figure 17 showed the flow rate of the two columns converged after 21 hours, and then diverged to a constant level.

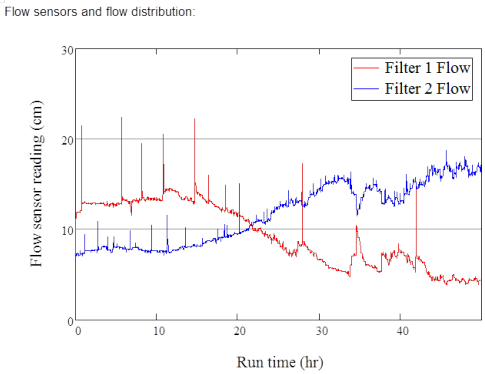


Figure 17: Head loss of both columns of Result 4 for Equal Sand test

According to Figure 18, the head loss displayed a same increase or decrease trend as run time went by. Compared with Result 4, the head loss of the two columns in this case, had a relatively big difference at the beginning of the experiment, and the difference became bigger with the run time passing by.

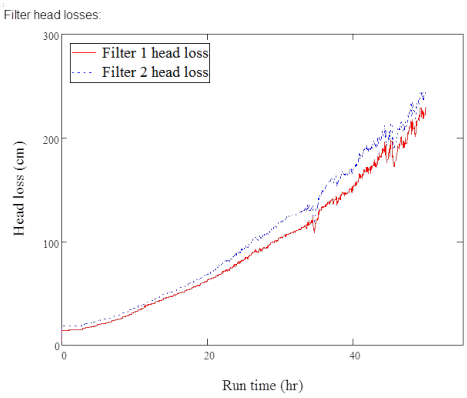


Figure 18: Head loss of both columns of Result 4 for Equal Sand test

## Unequal Sand Tests

### Result 1

This experiment ran for around 16 hours with clean incoming water.

According to Figure 19, the flow initially diverged and then started to approach to a steady state. The head loss (Figure 20) for Column 2 is more than Column 1. From the spikes at about 12.8 hour appear on both graphs, we suspect that there may have been some air in the system which causes the sudden drop.

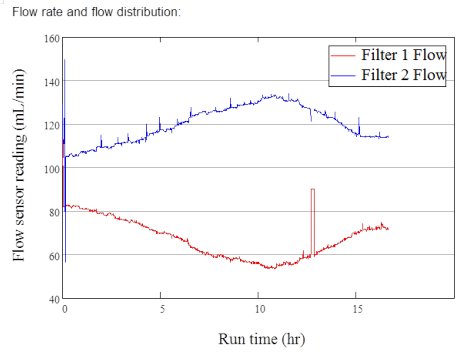


Figure 19: Flow rate of both columns of Result 1 for Unequal Sand test

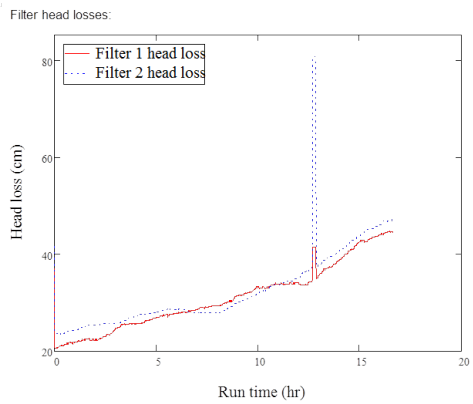


Figure 20: Head loss of both columns of Result 2 for Unequal Sand Test

**Result 2**

This experiment ran for around 4.5 hours with clean incoming water.

Flows of both columns (Figure 21) were about 10 mL/min apart and are consistent throughout the experiments. The head losses of both columns (Figure 22) are about 4 cm apart and are consistent throughout the experiments. From the order of spike occurrence in both columns, Filter 2 will respond to Filter 1 if there is an external disturbance in the system. It should be noted here, this is some good data for clean-bed flow distribution.

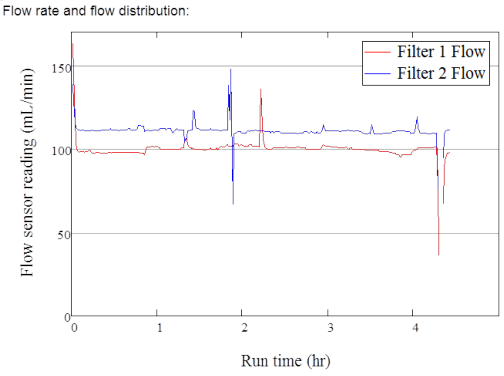


Figure 21: Flow rate of both columns of Result 2 for Unequal Sand test

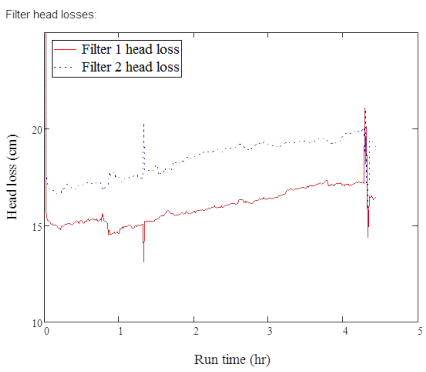


Figure 22: Head loss of both columns of Result 2 for Unequal Sand Test

### Result 3

This experiment ran for more than 30 hours with 20 NTU raw water.

Uneven amount of flow were observed in both columns (Figure 23), then they start to diverge, and ultimately approach a steady state. Since after 24 hours, the sand might be clogged by the clay and thus caused overloading of the filter system, the data after 24 hours is useless.

Since the flow distribution got worse when we started adding alum and clay, it might be that uneven flow does not readily correct itself just because clay is being entrained in the filters. This sort of data seems to suggest that we should not let the sand control flow distribution by itself.

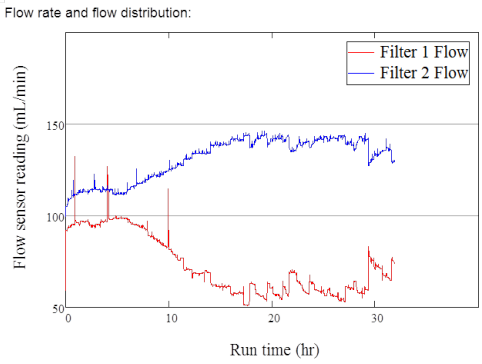


Figure 23: Flow rate of both columns of Result 3 for Unequal Sand test

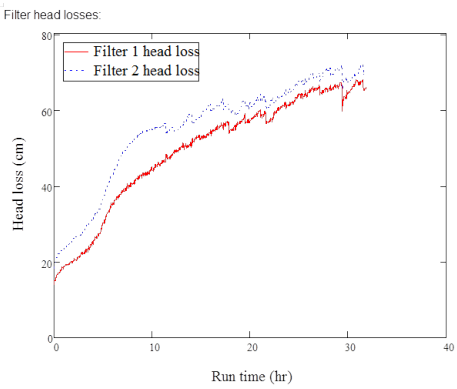


Figure 24: Head loss of both columns of Result 3 for Unequal Sand Test

## Depth Filtration Test

This depth filtration test used the modified apparatus whose incoming pipe was inserted about 2 cm deep into the sand layer. The experiment ran 24 hours with clean water, and another 24 hours with 20 NTU raw water and alum as coagulant. It should be mentioned here, the influent turbidity meter went wrong in this case, so the influent turbidity in the graph does not make sense.

Figure 25, Figure 26 and Figure 27 showed the result of turbidity, flow rate and head loss for both two columns respectively.

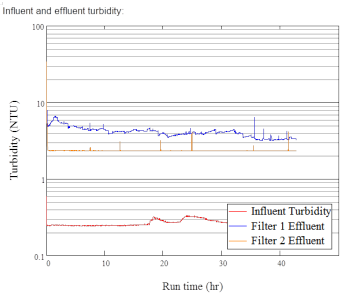


Figure 25: Flow distribution of both columns for Depth Filtration Test

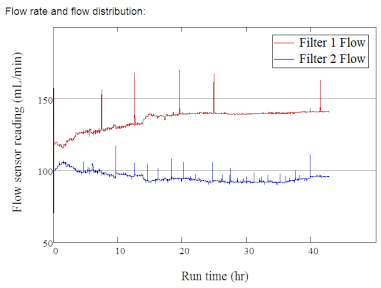


Figure 26: Flow rate of both columns for Depth Filtration Test

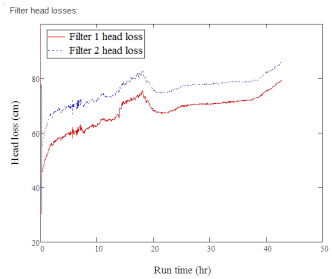


Figure 27: Head loss of both columns for Depth Filtration Test

From observations, air were trapped in both smaller tubes. After the clay and alum being pumped into the system at 24th hour, from Figure 26, we observed that the flow distribution kept relatively constant over the course of the remaining experiment. Figure 27 showed the head loss in the column increased much slower than the previous test. All these situations indicated that it was surface removal that dominated in the previous experiments.

## Effect of Energy Dissipation Rate

This part of the experiment is focusing on how do different energy dissipation rates affect the filter performance.

### Energy dissipation rate effect test

Figure 28 showed the relationship between the energy dissipation rate and the $pC^*$. In order to make the performance dimensionless, we use the pC* parameter which is defined as:

$$pC^* = -log\left(\frac{C}{C_0}\right) \tag{2}$$

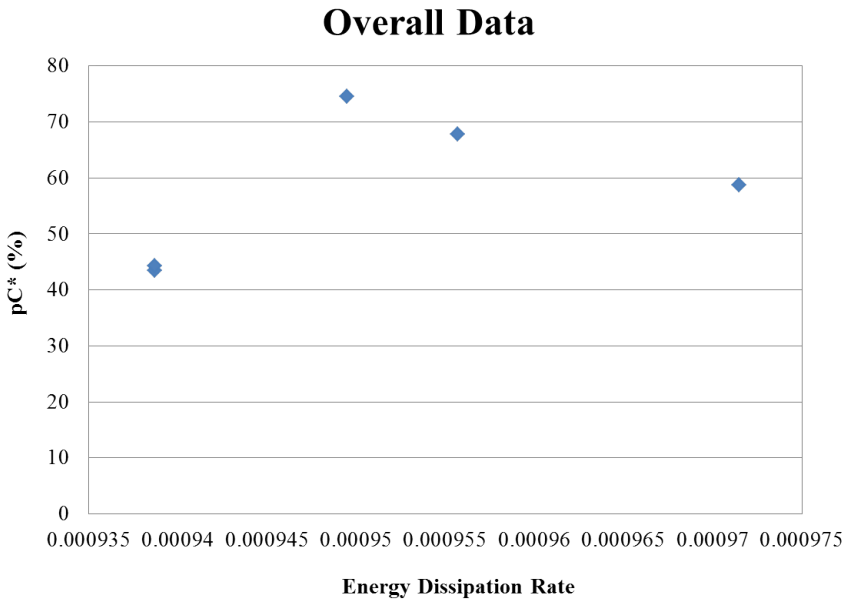


Figure 28: Relationship between the energy dissipation rate and the $pC^*$

Theoretically, with the increasing of energy dissipation rate, $pC^*$ would decrease correspondingly, and the results did generally suggest such a trend. Also, compared to previous test, the turbidity removal efficiency became lower.

### Valve Opened to Maximum

This experiment was ran with needle valve opened to maximum, with clay pumping at 0.28 mL/min, which yielded an influent turbidity as 25 NTU on average. Since there was no obvious cycle in the column, using MathCAD given initial average needle valve head loss of 0.000477 cm, the calculated diameter of the orifice is 3.983 mm, the jet velocity is 0.039 m/s, and the energy dissipation rate is $9.385 \times 10^{-4} m^2/s^3$.

Figure 29, 30, 31, and 32 showed the readings of turbidity, needle valve head loss, flocculation head loss, and column head loss, over the experiment cycle.

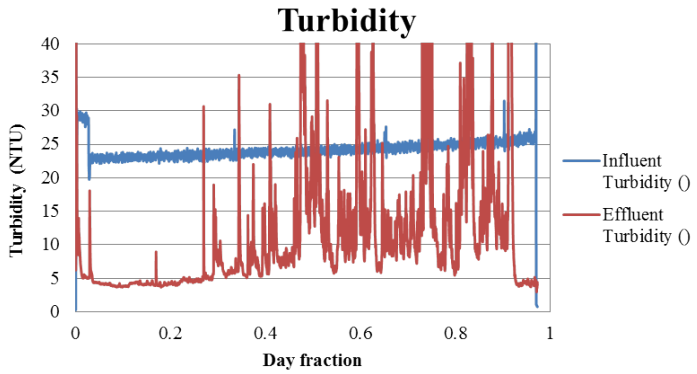


Figure 29: Turbidity for Influent and Effluent

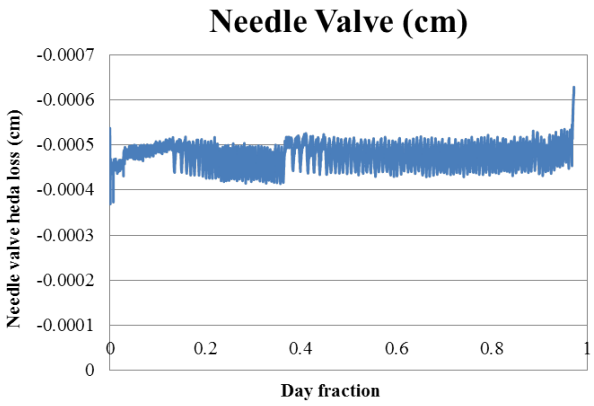


Figure 30: Needle Valve Head Loss

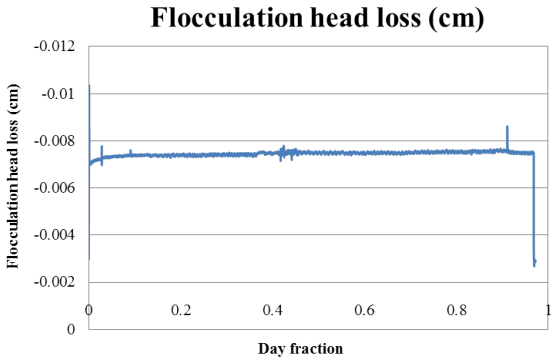


Figure 31: Flocculation Head Loss

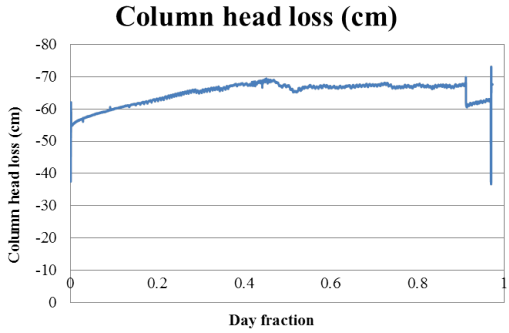


Figure 32: Column Head Loss

It it shown that the system was pretty stable, since the flocculation head loss was constant, with the head loss at the needle valve oscillated. By comparing the influent turbidity and effluent turbidity, it shows that at the first five hour, the percent of removal was stable, at about 75% removal. The head loss of the column increased almost linearly at the first 12 hours, and subsequently decreased and stayed almost at the same level.

### Valve Opened to Minimum

Valve was opened to the minimum the system could sustain, with clay pumping at 0.1 mL/min, which yielded an influent turbidity as 15 NTU on average. Since the system displayed several cycles in the test, using MathCAD given initial average needle valve head loss for every cycle, calculated the diameter of orifice, the jet velocity, the energy dissipation rate and in Table 1 below.

Figure 33, 34, 35, and 36 showed the readings of influent and effluent turbidity, needle valve head loss, flocculation head loss, and column head loss, over

| | Orifice Diameter $(mm)$ | Jet Velocity $(^{m}/_{s})$ | Average Needle Valve $\left(\times 10^{-3} cm\right)$ | Energy Dissip |
|---|---|---|---|---|
| Cycle #1 | 3.963 | 0.039 | 0.67 | |
| Cycle #2 | 3.956 | 0.039 | 0.74 | |
| Cycle #3 | 3.925 | 0.040 | 1.05 | |
| Cycle #4 | 3.909 | 0.040 | 1.22 | |
| Cycle #5 | 3.909 | 0.040 | 1.22 | |

Table 1: Calculated parameter for minimum valve case

the experiment cycle.

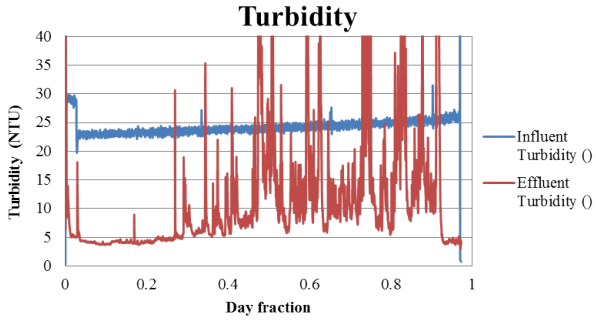


Figure 33: Influent and Effluent Turbidity

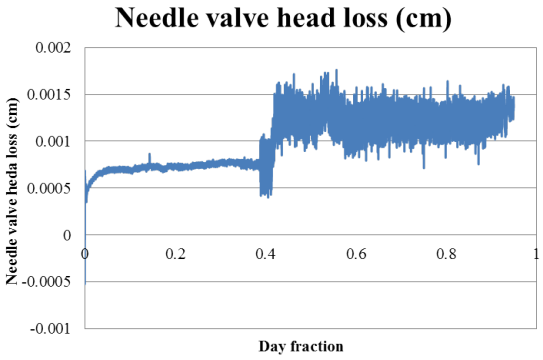


Figure 34: Needle Valve Head Loss

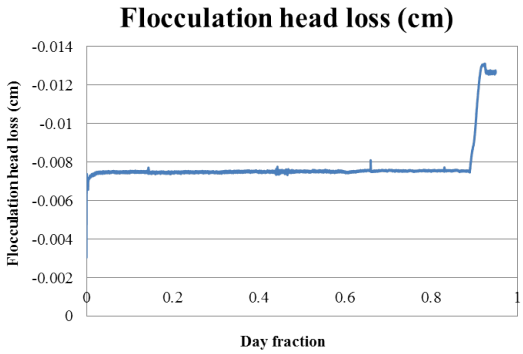


Figure 35: Flocculation Head Loss

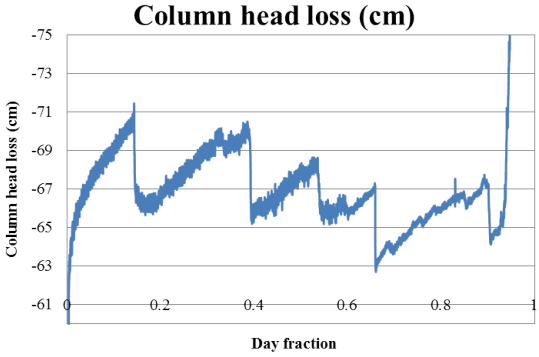


Figure 36: Column Head Loss

The percent removal for this experiment has a lot of uncertainties in it, since the effluent turbidity oscillated a lot, with a minimum turbidity around 4 NTU. The head loss for the needle valve and column head loss were increasing over the experiment, with a fairy constant flocculation head loss.

### Overall Performance

By plotted the energy dissipation rate versus pC*, as shown in Figure 37, we found that the overall performance of our experiment was not profound, with a 0.75 as the highest pC*. As the energy dissipation rate increases, the filtration performance starts to decrease in a almost linear manner at $9.495 \times 10^{-4} m^2/s^3$.

Figure 37: Energy Dissipation Rate vs. Performance

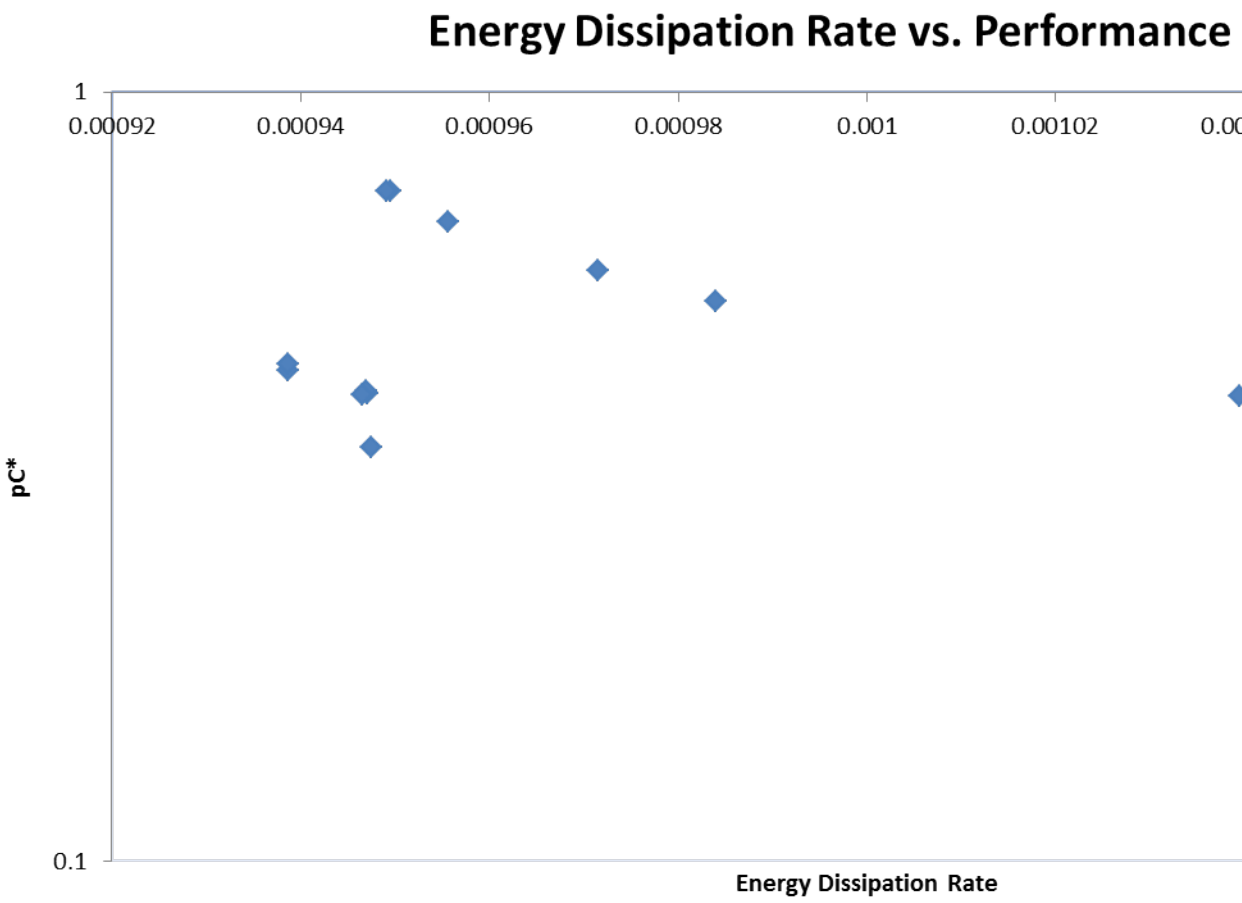

# Conclusion

**Self-healing testFrom the self-healing test, it seems clear that (1) even flow distribution is pretty hard to do if we just let the sand bed control what the flow distribution will be, and (2) this does NOT get better when we add alum and clay, for reasons that may have to do with performance as a function of filtration velocity and surface removal. All of this may suggest that we use hydraulic control of the flow distribution - that is, have outlet manifolds in the real filter with higher head losses, to promote more uniform distribution of flow among the layers.**

**Depth filtration test** Through the depth filtration test, we could see that surface removal was dominant in the first part of our experiment, which has affected the maximum run time of the filtration. On the other hand, the shape for surface removal on the head loss curve was eliminated, and the overall experiment is more stable by looking at the change in scale. Therefore, we concluded that surface removal will play an important role in filtration if water enters from the top of the sand column. This may affect the performance of conventional rapid-sand filters where all flow enters from the top of the sand bed, but SRSF may eliminate this effect by injecting flow straight into the sand bed. This experiment showed that direct injection of flow into the bed reduces surface removal and improves flow distribution.

**Energy dissipation rate test** From the energy dissipation rate test, we can see that the higher the energy dissipation rate before entering the filter column, the performance of the filter will decrease. Especially in the extreme case where valve diameter was opened to 2.992 mm, the whole experiment ran for about 5 hours only, then the column head loss reached its maximum, where sand bed was lifted. On the other hand, with the extreme case, the percent removal of the filter column was uncertain, and the sand column head loss will increase linearly. By comparing the results for different energy dissipation rate, we can conclude that the filtration removal will be more consistent, the column head loss and the needle valve head loss will be more stable over the filtration process. However, we need more data to support this conclusion.

# Future Work

Continue on with the current experiment with different energy dissipation rates. On the other hand, take a look at the data logging for beedle valve head loss to make sure it is logging the right unit, since the current data suggested a too small value for energy dissipation rate.

# References


[1] Monroe Weber-Shirk (2011), Filtration Theory course material for CEE 4540, Cornell University.

[2] Baumann, E.R., and Oulman, C.S. (1970),Sand and Diatomite Filtration Practices, In Water Quality Improvement by Physical and Chemical Processes, E.F. Gloyna and W.W. Eckenfelder, eds., University of Texas Press, Austin.

[3] Ian Tse, Karen, Monroe, and Len(2011), Fluid shear influences on the performance of hydraulic flocculation systems

[4] Denis Bouyer and Alain Line,Experimental Analysis of Floc Size Distribution under Different Hydrodynamics in a Mixing Tank,Published online in Wiley InterScience